⌘ *Author's Choice*

THE JOURNAL OF BIOLOGICAL CHEMISTRY VOL. 286, NO. 31, pp. 27729–27740, August 5, 2011

Engineered Bivalent Ligands to Bias ErbB Receptor-mediated Signaling and Phenotypes*[S]

Received for publication, January 12, 2011, and in revised form, May 26, 2011 Published, JBC Papers in Press, May 26, 2011, DOI 10.1074/jbc.M111.221093

Steven M. Jay[‡§¶1,2], Elma Kurtagic[‡1], Luis M. Alvarez[‡1,3], Seymour de Picciotto[‡1], Edgar Sanchez[‡], Jessica F. Hawkins[¶], Robin N. Prince[‡¶], Yadir Guerrero[‡], Carolyn L. Treasure[¶], Richard T. Lee[§¶4], and Linda G. Griffith[§¶‖4,5]

From the [‡]Department of Biological Engineering and [‖]Center for Gynepathology Research and Koch Institute for Cancer Research, Massachusetts Institute of Technology and the [§]Harvard Stem Cell Institute, Cambridge, Massachusetts 02139 and the [¶]Cardiovascular Division, Department of Medicine, Brigham and Women's Hospital, Harvard Medical School, Boston, Massachusetts 02115

The ErbB receptor family is dysregulated in many cancers, and its therapeutic manipulation by targeted antibodies and kinase inhibitors has resulted in effective chemotherapies. However, many malignancies remain refractory to current interventions. We describe a new approach that directs ErbB receptor interactions, resulting in biased signaling and phenotypes. Due to known receptor-ligand affinities and the necessity of ErbB receptors to dimerize to signal, bivalent ligands, formed by the synthetic linkage of two neuregulin-1β (NRG) moieties, two epidermal growth factor (EGF) moieties, or an EGF and a NRG moiety, can potentially drive homotypic receptor interactions and diminish formation of HER2-containing heterodimers, which are implicated in many malignancies and are a prevalent outcome of stimulation by native, monovalent EGF, or NRG. We demonstrate the therapeutic potential of this approach by showing that bivalent NRG (NN) can bias signaling in HER3-expressing cancer cells, resulting in some cases in decreased migration, inhibited proliferation, and increased apoptosis, whereas native NRG stimulation increased the malignant potential of the same cells. Hence, this new approach may have therapeutic relevance in ovarian, breast, lung, and other cancers in which HER3 has been implicated.

Members of the epidermal growth factor receptor (EGFR[6]/HER/ErbB) family, EGFR, HER2, HER3, and HER4, regulate diverse cell behaviors. The growth of many cancers is driven by mutation or overexpression of these receptors or their ligands (1, 2). Thus, numerous therapeutics directed at blocking signaling by this receptor family are in clinical development or use (1, 3–8). Overwhelming evidence supports the concept that ligand-induced activation of HER family members requires dimerization or oligomerization (1, 2, 9–11). Family members EGFR, HER3, and HER4 each have multiple known ligands, which are often produced in autocrine fashion to regulate cellular homeostasis or stress responses (12, 13). Although HER2 lacks known ligands, it heterodimerizes with other family members to form potent signaling complexes (10, 14). HER2 overexpression is found in up to 30% of breast cancers (4, 14), where contributions to the malignant phenotype are attributed at least in part to heterodimerization with HER3 (7, 14), which has a weak or inactive kinase but signals as a scaffold in partnership with other receptors (15, 16). Furthermore, in cancers of lung, breast, brain, and neck, where overexpression and/or mutation of EGFR are involved, interactions with HER2 or HER3 are often implicated in driving malignancy (14, 17). Thus, targeted disruption of particular dimers of ErbB receptors has been extensively explored for cancer therapy (6, 7); however, such strategies generally work only in a subset of patients, and resistance often emerges (4, 17–19). The mixed success of these approaches in clinical outcomes underscores the complexity of interactions and adaptations in the EGFR family signaling network and the need for additional tools and approaches for perturbing the network.

Although multivalency is not a recognized feature of HER family ligands, it drives receptor oligomerization in other receptor systems, such as the CD95/FasL system (20). We speculated that bivalent HER family ligands might be a broadly useful approach to manipulate HER family receptor associations. We created a panel of bivalent ligands by linking together two neuregulin-1β (NRG) moieties (ligand for HER3 and HER4), two epidermal growth factor (EGF) moieties (ligand for EGFR), or an EGF and a NRG moiety via a protease-resistant spacer of sufficient length to allow the two ligands to bind sites in adjacent (dimerized) receptors (Fig. 1*A*). These bivalent ligands may thus serve to drive particular homotypic or heterotypic receptor interactions (dimerization, oligomerization, or other modes of association) at the expense of others, thus functionally altering signaling and phenotypic outcomes compared with their native, monovalent counterparts.

* This work was supported, in whole or in part, by National Institutes of Health Grants AG032977 (to R. T. L.), DE019523 (to L. G. G.), EB003805 (to L. G. G. and R. T. L.), and U54-CA112967 (to L. G. G. via D. A. Lauffenburger). This work was also supported by the Army (Armed Forces Institute for Regenerative Medicine (to L. G. G.). Brigham and Women's Hospital and the Massachusetts Institute of Technology have filed for patents pertaining to the described bivalent ligand technology, listing L. M. A., S. M. J., R. T. L., and L. G. G. as inventors.

[S] The on-line version of this article (available at http://www.jbc.org) contains supplemental Table S1 and Figs. S1–S9.

⌘ *Author's Choice*—Final version full access.

[1] These authors contributed equally to this work.

[2] Supported by United States Department of Defense Breast Cancer Research Program Postdoctoral Fellowship W81XWH-11-1-0035.

[3] Supported by the Fannie and John Hertz Foundation (Livermore, CA) and the United States Army.

[4] Both are co-senior authors.

[5] Supported by the Radcliffe Institute for Advanced Studies. To whom correspondence should be addressed: MIT Biological Engineering, 77 Massachusetts Ave., Rm. 16-429, Cambridge, MA 02139. Tel.: 617-253-0013; Fax: 617-253-2400; E-mail: griff@mit.edu.

[6] The abbreviations used are: EGFR, EGF receptor; NRG, neuregulin-1β; NSCLC, non-small cell lung carcinoma; hTMSC, human mesenchymal stem cells; E_N, EGF; N_N, NRG; E_C, EGF; N_C, NRG; NN, N_CN_N; EE, E_CE_N.

We applied these new tools to test the hypothesis that a bivalent ligand incorporating two HER3 ligand moieties might drive stable, unproductive homotypic association of HER3, thereby sequestering ligand-bound HER3 from undesirable signaling partnerships, especially with HER2 (Fig. 1*B*). HER3 has emerged as a nexus for funneling malignant signals from EGFR, HER2, and c-MET into the PI3K/Akt pathway (16). Because HER3 has weak kinase activity (15), homotypically associated HER3 may be incapable of activating downstream signaling pathways. We show here that a HER3 binding bivalent NRG ligand (NN) induces differential behavior in numerous cancer cell lines compared with native, monovalent NRG. In some cases treatment with NN resulted in suppression of malignant phenotypes; thus, sequestration of HER3 using NN may represent a novel therapeutic modality for HER3-dependent cancers.

EXPERIMENTAL PROCEDURES

Protein Production and Characterization—Coding DNA for fusion proteins (as shown in supplemental Table S1) consisting of human sequences of EGF or NRG domains, protease resistant hydrophilic spacers, and heterospecific coiled coil domains were designed *in silico* (VectorNTI) and ordered as whole gene products with an *Escherichia coli* codon bias from GeneArt (Regensburg, Germany). Coding sequences were amplified by PCR mutagenesis with flanking restriction sites to permit cloning into pMAL-c2X (New England Biolabs) expression vectors. All expression constructs were sequenced before transformation into the *E. coli* expression strain BL21(DE3)pLysS (Stratagene). Transformed strains were initially grown to an optical density ~0.6 with agitation at 37 °C, then brought to 25 °C, and protein expression was induced with a single pulse of 100 nM IPTG for 4 h. Protein was harvested after cell lysis with BugBuster MasterMix (Novagen) supplemented with PMSF and protease inhibitor mixture (Sigma). Lysates were clarified by centrifugation at 3500 × *g* for 1 h at 4 °C. Clear lysate was subjected to purification on amylose resin and Factor Xa cleavage in accordance with manufacturer's protocol. Purified proteins were analyzed by Coomassie staining of SDS-PAGE, immunoblotting, and mass spectrometry. Coomassie staining revealed a single purified band for all proteins, as confirmed by mass spectrometry. Immunoblots confirmed the presence of full-length protein when probed for terminal epitopes. Binding-deficient versions of E_C and E_N were derived from previously described EGF mutant XVI (21) and were created via using a site-directed mutagenesis kit (Qiagen). Bioactivity of purified fractions was confirmed by *in vitro* cell response *versus* native ligands EGF and NRG-1β (Peprotech). Specificity for HER receptor activation was assessed using the pan-HER kinase inhibitor *N*-(4-((3-chloro-4-fluorophenyl)amino)pyrido[3,4-d]pyrimidin-6-yl)2-butynamide (Calbiochem #324840).

Validation of Coiled Coil Interaction—Coiled coil interactions between heterospecific pairs (*i.e.* $E_C + E_N$, $E_C + N_N$, and $N_C + N_N$) were characterized via an immunofluorescent binding assay as described in Moll *et al.* (22), with similar results. Controls included non-biotinylated ligand to measure nonspecific adsorption and staining of biotinylated ligand with secondary antibody to control for variations in bound ligand, and data were fitted to a one-parameter binding isotherm, revealing a sub-pM affinity. Coiled coil binding was also confirmed by far Western blotting by spotting 0.5 μl of sample ligand binding partner and controls in duplicate at 1 mM concentration onto a nitrocellulose membrane that was pre-wetted with 1× transfer buffer (4:1 MilliQ water:methanol and MES buffer). Membranes were washed 3 times with 20 mM Tris-buffered saline + Tween 20, pH 7.4 (TBST), then blocked for 1 h with blocking buffer (OBB, Licor Odyssey). Biotinylated cognate binding proteins were then added to the blocking buffer at 100 nM and incubated overnight at 4 °C. The membranes were then washed 3× with TBST, probed for 1 h with IR dye-conjugated streptavidin (Rockland) diluted 1:10,000 in OBB, washed 3× in TBST, and scanned on a Licor Odyssey IR scanner. Coiled coil binding was also confirmed by surface plasmon resonance on a Biacor2000 instrument using a streptavidin-coated gold analysis chip. Biotinylated E_C (or N_C) was immobilized on the chip surface and brought to equilibrium with running buffer. The conjugation of E_C (or N_C) to the chip surface exhibited a stable base line within 90 s of flowing E_C (or N_C) and remained stable over long buffer wash times, indicating a stable surface binding of E_C (or N_C). Attempts to conjugate additional E_C (or N_C) showed no change in base line, indicating saturation of the chip surface. Cognate binding partner E_N (or N_N) was flowed over the surface, and binding signal was collected.

Cell Lines—Human telomerase reverse transcriptase-immortalized human mesenchymal stem cells (hTMSC) were a gift from Dr. Junya Toguchida (Kyoto University, Kyoto, Japan). HeLa cells were obtained from ATCC. HeLa and hTMSC were maintained in Dulbecco's modified Eagle's medium (DMEM) containing 10% fetal bovine serum (FBS), 1% L-glutamine, 1% non-essential amino acids, 1% sodium pyruvate, and 1% penicillin/streptomycin. MCF-7 cells were obtained from ATCC and were maintained in phenol red-free medium of the same composition. All cell culture media and additives were purchased from Invitrogen. For single-cell migration studies, hTMSC were maintained in a DMEM medium containing 0.5% dialyzed fetal bovine serum (FBS), 1% L-glutamine, and 1% penicillin/streptomycin at 37 °C, 95% humidity, and 5% CO_2. H3255 and H1975 cells were a generous gift of Dr. Pasi Janne (Dana Farber Cancer Institute). H1975 cells were cultured in RPMI 1640 media with 10% FBS, 5 mM L-glutamine, 100 units/ml penicillin G, 100 μg/ml streptomycin. H3255 cells were cultured in RPMI 1640 plus the 10% FBS, 0.02 mg/ml insulin, 0.01 mg/ml transferrin, 25 nM sodium selenite, 50 nM hydrocortisone, 1 ng/ml epidermal growth factor, 0.01 mM ethanolamine, 0.01 mM phosphorylethanolamine, 100 pM triiodothyronine, 0.5% (w/v) bovine serum albumin, 0.5 mM sodium pyruvate, 5 mM L-glutamine, 100 units/ml penicillin G, 100 μg/ml streptomycin. H1299 cells were purchased from ATCC and maintained in RPMI 1640 media with 10% FBS, 5 mM L-glutamine, 100 units/ml penicillin G, 100 μg/ml streptomycin. MDA-MB-435 transductants were a generous gift of Dr. Jeffrey Segall (Albert Einstein College of Medicine) and were cultured as described (23). MDA-MB-453 cells were a generous gift of Dr. Michael Yaffe (Massachusetts Institute of Technology) and were cultured in DMEM media with 10% FBS, penicillin/streptomycin, and L-glutamine.

Cell Signaling and Migration—HER4 inhibition experiments in MCF-7 cells were performed after seeding into 12 well plates at 250,000 cells per well in serum containing medium and incubation for 48 h. Cells were then serum-starved for 5 h before ligand treatment. Anti-HER4 antibody clone H4.72.8 (Millipore #05-478) was then added to the cells at 10 μg/ml 30 min before subsequent treatments. IC_{50} measurements were made by dosing cells with concentrations of bivalent NN ligand in the range of 1 μM to 1 fM for 10 min followed by a pulse of 3 nM NRG for an additional 10 min. This dose of NRG and end point time were validated by generating a NRG dose response curve for MCF-7 cells in the concentration range 1 μM to 1 fM for 20 min. 3 nM NRG was the lowest dose that produced near maximal pERK1/2 signal at 20 min. After all stimulation experiments, cells were placed on ice, and medium was aspirated, washed with ice-cold PBS, and lysed with lysis buffer (Calbiochem #FNN0011).

For Western blotting, membranes were probed with primary antibodies (9106 pERK1/2, 2236 pEGFR, 9271 pAkt, 2241 pHER2, 21D3 pHER3, 4267 EGFR, 2242 HER2, all from Cell Signaling Technology; sc-415 HER3 from Santa Cruz Biotechnology, ab63354 HER4 from Abcam) and secondary IR-Dye conjugate antibodies (IR-Dye700/800, Rockland) and scanned using a Licor Odyssey IR scanner (Licor Systems, Inc.). Quantification of phosphorylated (pY) EGFR, HER2, and ERK1/2 was carried out using Widescreen® (EMD Biosciences) and Bioplex® bead kits according to the manufacturer's instructions. Readouts were made on a Bioplex 200 System (Bio-Rad, Luminex Technology). Linearity of the pYpanEGFR and pERK1/2 assays was checked using varying ratios of stimulated lysates from hTMSC or HeLa cells, and results were used to determine the optimal loading per well. Where indicated, anti-HER4 antibody H4.72.8 was added to cells at 10 μg/ml 30 min before subsequent treatments.

For transwell migration experiments, hTMSC were seeded in HTS Fluoroblock transwell well chambers (BD Biosciences) in DMEM + 10% FBS medium and mitomycin-C (Calbiochem). Cells were fixed, stained, and quantified after 18 h. The upper chambers were emptied of medium and filled with 4% formaldehyde solution, washed 2× with PBS, then incubated in SYTO 16 nuclear stain (Invitrogen) for 15 min. These were again washed with PBS and then placed in a clean 24-well plate and read using a SpectraMax M2e multi-well fluorescent plate reader (Molecular Devices Corp.). A standard curve correlating fluorescence with cell number was obtained by plating known numbers of cells in a 12-well plate in culture medium containing mitomycin-C. Standard cell numbers were confirmed by a ViCell hemocytometer (Beckman-Coulter).

For assessment of single cell chemokinesis, H1975 cells were labeled with 10 μM of Celltracker Green CMFDA (Invitrogen) and seeded at 4000 cells/cm^2 on a 5 μg/cm^2 fibronectin-coated glass bottom 24-well dish (Mattek, Inc) in serum-free medium overnight. Anti-HER4 antibody clone H4.72.8 was added to the cells at 10 μg/ml 30 min before subsequent ligand treatments. Time lapse images were taken every 10 min for 12 h using a BD CARVII spinning disk confocal with an Axio Observer Zeiss microscope equipped with environmental control (37 °C, 5% CO_2). The "spots" function in Imaris (Bitplane, Zurich, Switzerland) was used to calculate cell centroids, and migratory tracks of individual cells were generated using the Brownian motion tracking algorithm. All generated tracks were then manually verified for accuracy and modified when the automated logarithm presented errors. Cells undergoing division, death, as identified as the release of fluorescence, or blebbing were not tracked. Wind-rose plots were generated from the tracks produced from 30 randomly chosen cells from the motile population and overlaying the starting coordinates at the origin of the plots to graphically represent average cell dispersion during migration.

To assess chemotaxis in MDA-MB-435 cells overexpressing HER2 (MDA-MB-435-HER2), chambers were precoated for 2 h at 37 °C with 20 μg/ml fibronectin. Cells were serum-starved for 2 h and seeded at 20,000 cells/well in MEMα media with 0.35% bovine serum albumin (BSA) on top of chemotaxis chambers (Neuro Probe, ChemoTx® Disposable Chemotaxis System, #101-8, 8-μm pore size). Ligands were placed in the media of the upper and lower chamber, whereas a gradient of recombinant human neuregulin-1 (Peprotech) was formed by dosing to 1 nM in the lower chamber only. The chemokinesis control had 1 nM recombinant human neuregulin-1 in the upper and lower chambers. After 4 h, non-migrated cells were wiped from the top, and the chamber was washed with PBS, allowed to dry, and frozen at −80 °C. Cells that migrated across the membrane were quantified via the CyQuant assay (Invitrogen).

Non-small Cell Lung Carcinoma (NSCLC) Cell Proliferation and Apoptosis—H3255 cells were seeded at 6000 cells per well in 96-well plates overnight in complete media. Subsequently, media were changed to serum-free (unless noted) media containing designated doses of ligands, and the cells were incubated an additional 48 h. Cell proliferation was assessed using the CyQUANT-NF proliferation kit (Invitrogen). All other proliferation experiments were carried out identically, with the exception of initial seeding at 3500 cells/well for all cells except MDA-MB-453, which were seeded at 2500 cells/well. For apoptosis studies, H1975 cells were seeded in chamber slides (Nunc, Rochester, NY) at 50,000 cells/cm^2. 24 h later media were aspirated and replaced by new media with and without N_C (100 nM) or bivalent NN (100 nM) and incubated for additional 24 h. Caspase-3 was detected using a NucViewTM Caspase-3 Assay kit for live cells according to the manufacturer's protocol. For competition studies, all ligands were dosed simultaneously.

Receptor Binding and Aggregation—Binding assays were facilitated by radiolabeling N_C with ^{125}I using the Bolton-Hunter reagent (PerkinElmer Life Sciences) using standard methods. Binding to ErbB3 extracellular domains was performed by incubating a range of ^{125}I-N_C or ^{125}I-NN concentrations (0.1, 0.25, 0.5, 1, and 3 nM) with Fc-ErbB3 chimeras (R&D Systems, Minneapolis, MN) (0.1 nM) in binding buffer (25 mM HEPES, pH 7.4, 150 mM NaCl and 1 mg/ml BSA) for 3 h at 4 °C. The bound complexes were pulled down with magnetic protein-A beads (New England Biolabs, Beverly, MA). The beads were washed three times with binding buffer, and ^{125}I-N_C or ^{125}I-NN associated with the beads was measured using a Coba Auto-Gamma 5005 (Packard Instruments, Meridian, CT). For binding to MCF-7 cells, which express NRG receptors HER3 and HER4, cells were plated at a density of 8 × 10^4/well in 24-well plates and grown to confluence. Cells were then washed

with ice-cold binding buffer (25 mM HEPES, pH 7.4, in serum-free RPMI containing 1 mg/ml BSA) and incubated for 10 min at 4 °C to inhibit endocytosis and binding site turnover. ^{125}I-N_C or ^{125}I-NN with and without an excess amount of unlabeled N_C/NN or unlabeled recombinant human NRG (Peprotech) (500 nM) were added to the cells and incubated for 3 h at 4 °C. Unbound ligands were washed 3× with binding buffer, and bound ligands were extracted with 10 mM Tris, pH 7.4, 1 mM EDTA, 0.5% SDS for 15 min at room temperature. ^{125}I-Labeled protein was quantified using a γ-counter (Coba Auto-Gamma 5005).

ErbB3 aggregation was measured via the change in hydrodynamic radius using a DynaPro Titan Dynamic Light Scatterer. Receptor (soluble chimera Fc-ErbB3 extracellular domain, as above) and ligands were allowed to interact overnight at 4 °C, 20 μl of sample were loaded into a frosted cuvette, and 10 10-s readings were recorded. Data were normalized to the radius of receptor alone.

Cellular Imaging—For imaging studies, glass coverslips that were previously etched using sulfuric acid, sterilized, and coated with 3 μg/ml of human fibronectin (Sigma) in phosphate-buffered saline (PBS) were used. 1% (w/v) BSA (Sigma) in PBS was then added to each coverslip for 1 h to block any uncoated regions, and coverslips were washed before seeding with hTMSC at 4000 cells/cm^2 overnight (>16 h) in standard culture conditions (37 °C, 5% CO_2). Ligands were diluted to appropriate concentrations (100 nM) in quiescent media, and cells were stimulated with either EGF (E_N), EGF-EGF bivalent ligand (EE), or media alone for 2 min. Media was then aspirated, and cells were subsequently fixed with warm (37 °C) 4% formaldehyde solution in PHEM buffer (PIPES, HEPES, EGTA, and $MgSO_4$, pH 7.0) for 10 min at room temperature. A PBS wash removed any excess 4% formaldehyde. Nonspecific binding of antibodies was blocked by incubating the coverslips with blocking buffer (10% BSA in PBS) for 30 min before antibody exposure. The goat polyclonal IgG anti-EGFR (sc-03-g, Santa Cruz Biotechnology) and the Alexa Fluor 594 donkey anti-goat IgG (Invitrogen) were each diluted to working concentrations in blocking buffer. Coverslips were first exposed to the primary antibody (goat anti-EGFR) for 1 h at room temperature followed by 5 min washes with washing buffer (0.5% w/v BSA in PBS). The anti-goat IgG antibody incubation followed for 1 h at room temperature in the dark. Coverslips were stained with DAPI pro-long gold (Invitrogen), mounted, and sealed. Images were captured with a 60× objective (2 × 2 binning) on an Olympus IX71 inverted microscope using Softworx software for image acquisition.

Statistical Analysis—Data are presented as the mean ± S.E. unless otherwise indicated. Unless noted, statistical significance was determined based on two-way analysis of variance. Statistical significance for transwell migration was determined by Student's *t* test, and whereas statistical analysis of single cell migration was evaluated using a Kruskal-Wallis nonparametric test with a Dunn's post-test.

RESULTS

Design and Validation of Bivalent Ligands—To explore potential signal-biasing effects across the HER family, bivalent engineered ligands were constructed in a modular fashion (Fig. 1*A*) by synthesizing fusion proteins of monomeric ligands (NRG and/or EGF) with a protease-resistant spacer (24) and a high (fM) affinity coiled coil domain (22) using cloning, expression, and purification strategies described under "Experimental Procedures." Reports analyzing ligand binding to EGFR and HER3 suggested that receptor binding and activation would not be impaired by modification of either the N or C terminus (25–27). Bivalent ligands were designed using the crystal structure of the EGF-bound homodimerized extracellular domain of EGFR in which native ligands assume an anti-parallel orientation with respect to their termini and are separated by ~10 nm (28) (Fig. 1*A*). The EGF and NRG component protein designs were based on the same geometrical parameters given the close similarity in ligand structure and receptor/ligand interactions (25, 29). Thus, N-terminal modified constituents (EGF (E_N) or NRG (N_N)) could be joined to C-terminal modified constituents (EGF (E_C) or NRG (N_C)) through high affinity heterospecific coil interactions (see "Experimental Procedures"). Combination of these individual fusion proteins resulted in the bivalent ligands NRG-NRG (N_CN_N, abbreviated as NN), EGF-EGF (E_CE_N, abbreviated as EE), and EGF-NRG (EN), with EGF or NRG moieties separated by a flexible spacer of total length ~20 nm.

Monovalent N_N and N_C both activated ERK1/2 in a comparable fashion to NRG in the mammary tumor line MCF-7 (supplemental Fig. S1, *A* and *C*), which expresses both HER3 and HER4 (30–33) (supplemental Fig. S2). It is notable that although unstimulated MCF-7 cells express low (often undetectable by Western analysis) levels of HER4, as seen in supplemental Fig. S2, NRG-stimulation is reported to induce proliferation in these cells, resulting at least partially from signaling downstream of HER4-phosphorylation (34). Additionally, monovalent E_N and E_C activated ERK1/2 in a fashion comparable with EGF in HeLa cells (supplemental Fig. S1, *B* and *D*), which express both EGFR and HER2 (supplemental Fig. S2).

HER3 is a weak kinase that signals through interactions with other receptors, including HER2, and such interactions are associated with malignant phenotypes (7, 15, 35, 36). Unliganded HER3 is reported to exist in an autoinhibited, associated state on the cell surface (2, 25, 35, 37, 38). Native NRG does not induce homodimerization of HER3 (9, 39, 40) but, rather, appears to disrupt HER3 clusters. We predicted that NN ligands would opportunistically link adjacent HER3 into homotypic associations, sequestering HER3 from interactions with HER2 and other potential partners and thereby reducing both HER3 and HER2 activation (Fig. 1*B*). As an initial test system for this hypothesis, we used the NSCLC line H3255, which expresses HER3, HER2, and a mutant EGFR that cooperates with HER3 to activate PI3K/Akt and is not known to express HER4 (41) (supplemental Fig. S2). When H3255 cells were challenged with NRG (N_C), they exhibited a dose-dependent phosphorylation of both HER3 and HER2 (Fig. 1*C*). In contrast, NN failed to elicit similar activation of HER3 and HER2, stimulating slight phosphorylation only at low doses (Fig. 1*C*). This result is consistent with the proposed model of HER3 sequestration from HER2 by NN.

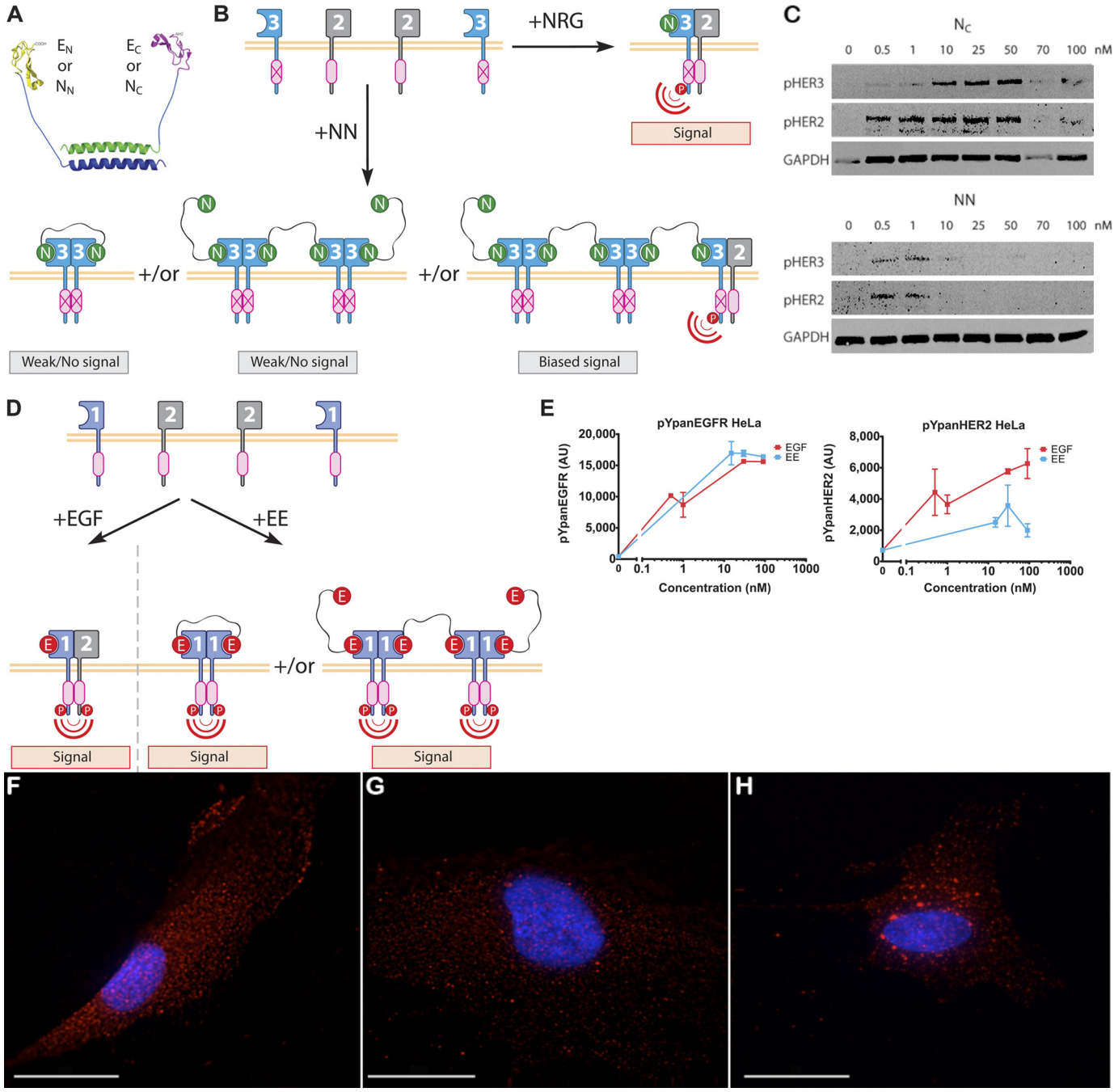

FIGURE 1. **Design and validation of bivalent ligands.** *A*, bivalent ligands were formed via heterospecific coiled coil interactions of N- or C-terminal modified EGF (E_N, E_C) or NRG (N_N, N_C) fusion proteins. Thus, formation of bivalent ligands with two EGF domains, two NRG domains, or one EGF and one NRG domain is possible. *B*, possible mechanisms for the observed differences in monovalent NRG compared with bivalent NN, in which NN fosters homodimerization or homo-oligomerization of HER3 at the expense of heterodimers with HER2, are illustrated in the schematic. *C*, Western analysis is shown of pHER2 and pHER3 in lysates from NSCLC line H3255 cells stimulated for 15 min by monovalent NRG (N_C) or bivalent NN (data are representative of two independent experiments). *D*, the schematic illustrates a model for EE binding that facilitates EGFR homodimerization or homo-oligomerization, leading to at least partial sequestration of EGFR from heterodimerization with HER2. *E*, HeLa cells were stimulated for 15 min with escalating doses of EGF or EE, lysed, and analyzed by Luminex technology for pan-pY-EGFR or pan-pY-HER2 ($n = 3$). *AU*, absorbance units. hTMSC were stimulated for 2 min with no ligand (*F*), 100 nM monovalent EGF (*G*), or 100 nM bivalent EE (*H*); cells were fixed, and EGFR receptors were identified by immunofluorescent staining (*red*). *F*, *G*, and *H*, nuclei were stained with DAPI (*blue*); *scale bar* = 30 μm, images are representative of 5 cells per condition ($n = 5$) from a representative experiment of 3 total.

We conducted several experiments to rule out the possibility that the relative lack of HER2 and HER3 activation in H3255 arose from failure of NN to bind specifically to HER3. Using ^{125}I-N_C, we established that NN binds to the HER3 extracellular domain (ECD) in a specific manner (supplemental Fig. S3*A*). Furthermore, bivalent NN - but not monovalent N_C, N_N, NRG, or bivalent EN - induced aggregation of the Fc-HER3 extracellular domain as assessed by dynamic light scattering (supplemental Fig. S3*B*). Aggregation is expected only if both moieties in the bivalent structure are competent to bind HER3, thus presumably inducing oligomerization of the preformed HER3 extracellular domain homodimers, and the failure of EN to

induce aggregation in this setting suggests that the effect requires both neuregulin domains of NN to bind to a HER3 domain on two different homodimers. We also determined that bivalent ^{125}I-NN exhibited specific binding to MCF-7 cells (supplemental Fig. S3*C*).

In contrast to HER3, EGFR homodimers are competent to signal. The presence of preformed EGFR homodimers or oligomers (42) may enable bivalent EE ligand to link proximal EGFR into homotypic interactions upon binding (Fig. 1*D*). We, therefore, predicted that stimulation of cells with EE would result in activation of EGFR and downstream pathways along with diminished activation of HER2 compared with stimulation with EGF. We first examined whether EE could activate signaling downstream of EGFR in a specific manner. 10 nM EE effectively stimulated ERK1/2 phosphorylation in HeLa cells, which express comparable levels of EGFR and HER2 (43–46), at levels similar to those observed by the constituent subunits E_C and E_N (supplemental Fig. S4). Additionally, binding-deficient versions of E_C and E_N were constructed by replacing a seven-amino acid sequence in the EGF domain with a seven-amino acid sequence from NRG (21). These proteins did not activate ERK1/2 at significant levels above background but also did not prevent ERK1/2 phosphorylation when paired with a complementary, non-binding deficient fusion protein (supplemental Fig. S4). Finally, combination of the binding-deficient EGF proteins to form a binding deficient (BD) bivalent construct (E_N-BD + E_C-BD) resulted in ERK1/2 phosphorylation at levels similar to background at 10 nM, indicating that signaling effects mediated by bivalent ligands are specific to the activity of their constituent members.

With evidence that EE activates signaling downstream of EGFR in a specific manner, we examined the relative activation of EGFR and HER2 in cells stimulated with monovalent compared with bivalent ligand. At saturating doses, EGF and EE activated EGFR in a comparable fashion in HeLa cells, but activation of HER2 was diminished by ~50% in cells stimulated with EE compared with EGF (Fig. 1*E*). This reduction of pHER2 is supportive of the hypothesis that EE partially sequesters EGFR in homotypic interactions, as illustrated schematically in Fig. 1*D*. We further hypothesized that, if EE does indeed drive EGFR homotypic interactions, clustering of EGFR on a cell surface may occur. To investigate the hypothesis, we assessed the distribution of EGFR on intact cells via immunofluorescent imaging. hTMSC cells stimulated with EE exhibited bright clusters of labeled EGFR (Fig. 1*H*), whereas the EGFR surface distribution on EGF-stimulated cells was diffuse (Fig. 1*G*), more closely resembling the receptor distribution of unstimulated hTMSC (Fig. 1*F*).

In summary, we established that the engineered bivalent ligands interact specifically with cell surface HER receptors and that these interactions appear to have significant effects on activation of these receptors compared with those induced by native HER receptor ligands. We predicted that treatment with NN might suppress malignant phenotypes driven by HER3-HER2 signaling; thus, we focused further investigations on this engineered protein.

Bivalent NN Induces Differential Intracellular Signaling Compared with Native NRG—HER3-HER2 receptor interactions lead to intracellular signaling cascades that are associated with many malignant behaviors (7, 15, 35, 36). We predicted that such pathways would not be activated if bivalent NN ligands sequester HER3 into homotypic interactions (Fig. 1*B*). In hTMSC, which express EGFR, HER2, and HER3 (47), stimulation with monovalent NRG (N_C) induced a robust dose-dependent phosphorylation until saturation at high doses of ERK1/2, which is a well characterized member of the mitogen-associated protein kinase family that regulates cellular programs such as proliferation, differentiation, and motility (Fig. 2*A*). In stark contrast, stimulation with bivalent NN resulted in a nearly complete lack of pERK1/2 above the unstimulated control condition (Fig. 2*A*). Additionally, N_C strongly induced phosphorylation of Akt, a serine/threonine protein kinase that regulates cell proliferation, apoptosis, transcription, and migration in a dose-dependent manner in H3255 cells (Fig. 2*B*). In contrast, bivalent NN did not induce Akt significantly above control levels in these cells. Thus, in H3255 cells, NN-driven cell surface receptor associations (Fig. 1*C*) appear to correspond to altered intracellular protein phosphorylation (Fig. 2*B*), indicating that NN can bias signaling in these cells.

Because NRG also binds to HER4, NN may interact with both HER3 and HER4 in cells that express both receptors. The MCF-7 cell line expresses both HER3 and HER4, with HER4 being expressed at higher levels than most characterized cell lines (30–34), and thus it is a useful model for analysis of HER4 contributions to signaling in cancer cells that co-express both receptors (48), as ligand binding to HER4 can be blocked with an antibody in parallel experiments. As expected, incubation of MCF-7 cells with N_C resulted in phosphorylation of both ERK1/2 and Akt (Fig. 2*C*). Activation of these two downstream signaling nodes was also observed when MCF-7 cells were pretreated by incubation with an antibody that blocks ligand binding to HER4 before stimulation with N_C (Fig. 2*C*), indicating a prominent role for HER3 in these signaling pathways. Bivalent NN also activated ERK1/2 and Akt in MCF-7 cells. This is not surprising, as HER4 can form signaling-competent homodimers (11), and such dimers may be induced by NN; alternatively, the cell surface distribution of HER4 before stimulation may involve proximity to other ErbB receptors, enabling NN to act as a de facto monomeric ligand inducing opportunistic heterodimerization with HER2 or EGFR. As expected by our findings in other cell lines lacking HER4 (Figs. 1*B* and 2, *A* and *B*), where NN failed to activate downstream pathways, phosphorylation of ERK1/2 and Akt after incubation with NN was greatly diminished when MCF-7 cells were pretreated with an antibody that blocks ligand binding to HER4 (Fig. 2*C*), suggesting that when HER4 is unavailable in these cells, NN binds to and sequesters HER3.

To provide additional evidence that NN can block HER3-mediated signaling, MCF-7 cells were incubated with or without HER4 blocking antibody (10 min), then with NN at doses 0.1–100 nM (10 min), and then challenged with a saturating dose of NRG. For cells treated with the HER4 blocking antibody, preincubation with NN before stimulation with N_C abrogated downstream signaling in a dose (of NN)-dependent man-

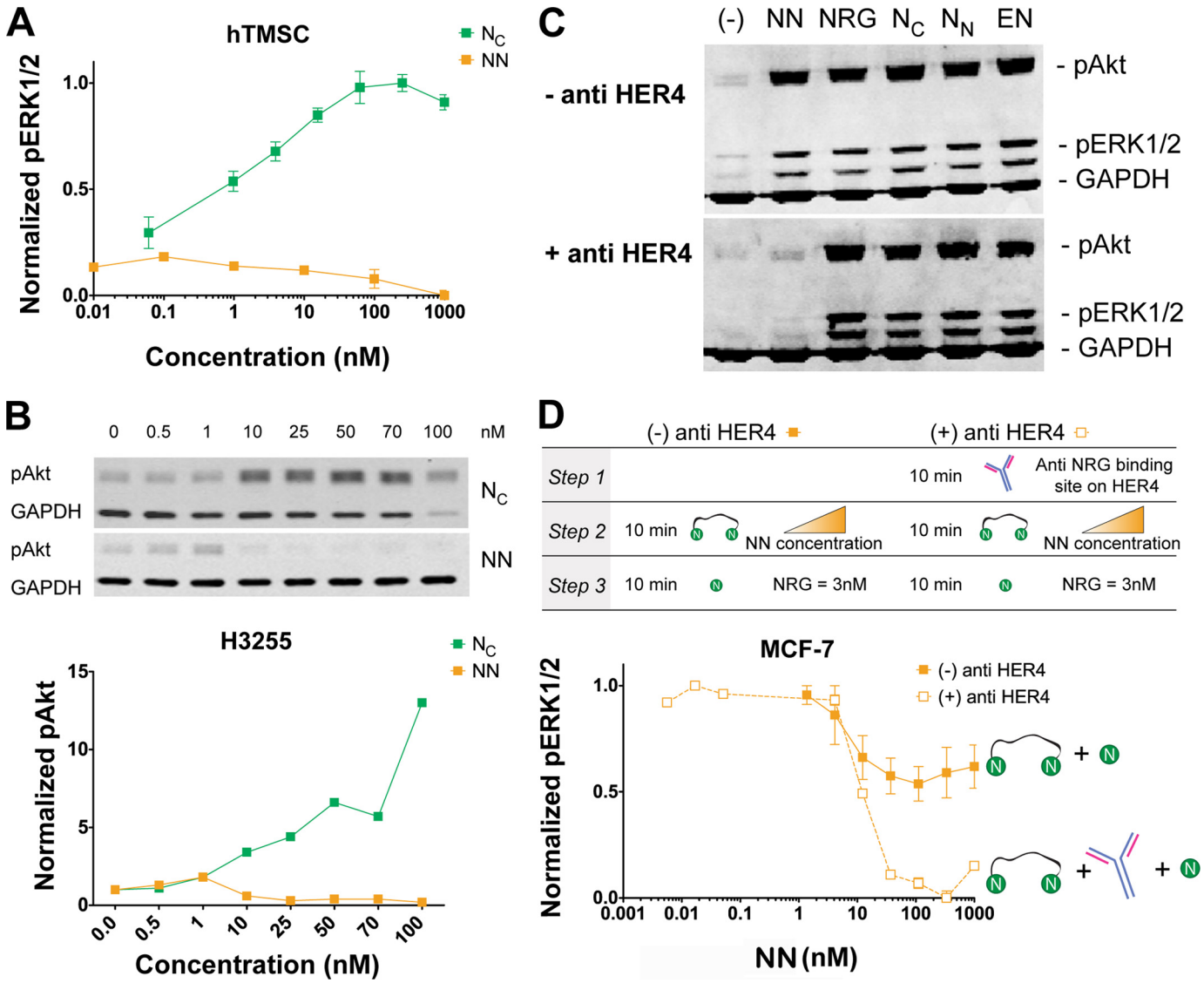

FIGURE 2. **Bivalent NN induces differential intracellular signaling compared with native NRG.** *A*, ERK1/2 phosphorylation was measured in hTMSC stimulated by monovalent NRG (N_C) and bivalent NN ($n = 8$, data displayed as mean ± S.D.) after 15 min. *B*, Akt phosphorylation was assessed in H3255 cells stimulated for 15 min by monovalent NRG (N_C) and bivalent NN. Quantification via densitometry is shown below (data representative of 2 independent experiments). *C*, MCF-7 cells incubated in the presence or absence of a HER4 blocking antibody were stimulated for 15 min with monovalent ligands NRG, N_C, or N_N, or bivalent ligands NN or EN, and ERK1/2 and Akt phosphorylation was assessed via Western analysis (data representative of three independent experiments; −, untreated controls). *D*, at the indicated time points, MCF-7 cells were incubated in the presence or absence of HER4 blocking antibody (anti-HER4) followed by NN stimulation and subsequent challenge with NRG. ERK1/2 phosphorylation was assessed by Western analysis ($n = 3$). Reference standards (normalized response = 1) for *A*, *B*, and *D* were set to the pERK1/2 level for 150 nM NRG (N_C), the pAkt level for untreated cells, and the pERK1/2 level for 1 nM NN (-anti-HER4, + 3 nM NRG)-treated cells, respectively.

ner with an IC_{50} of ~10 nM (Fig. 2*D*). This abrogation of signaling is consistent with our observation that NN competes with monovalent NRG in binding to MCF-7 cells (supplemental Fig. S3*C*) and suggests that it binds to and sequesters HER3 away from HER2 and other potential partners when HER4 is unavailable. Interestingly, ERK1/2 activation was also moderately attenuated in a dose-dependent fashion in the absence of HER4 blocking antibody (Fig. 2*D*), a finding that is arguably expected if the contributions of HER3 are silenced. Other factors, such as altered signaling by HER4 when liganded by NN, may also contribute.

Bivalent NN Inhibits Migration and Proliferation and Increases Apoptosis of Cancer Cells—NRG is known to stimulate cell migration via multiple mechanisms, including via HER2-HER3 heterodimers (23, 49–53). The inhibition of this signaling axis with small molecule inhibitors of HER2 has been shown to reduce cell migration (54). Thus, we hypothesized that sequestration of HER3 into homotypic interactions via NN might reduce migration. Indeed, upon the addition of NN, hTMSC chemotactic migration was significantly reduced compared with the control condition as well as to N_C-stimulated cells (Fig. 3*A*). Furthermore, in NSCLC line H1975, which expresses EGFR with the double mutation L858R and T790M as well as HER2 and HER3 (55), NN stimulation reduced chemokinesis relative to NRG-stimulated and untreated control cells (Fig. 3, *B* and *C*). Also, NRG-induced chemotaxis of MDA-MB-435 cells overexpressing HER2 (MDA-MB-435-HER2) was reduced in a

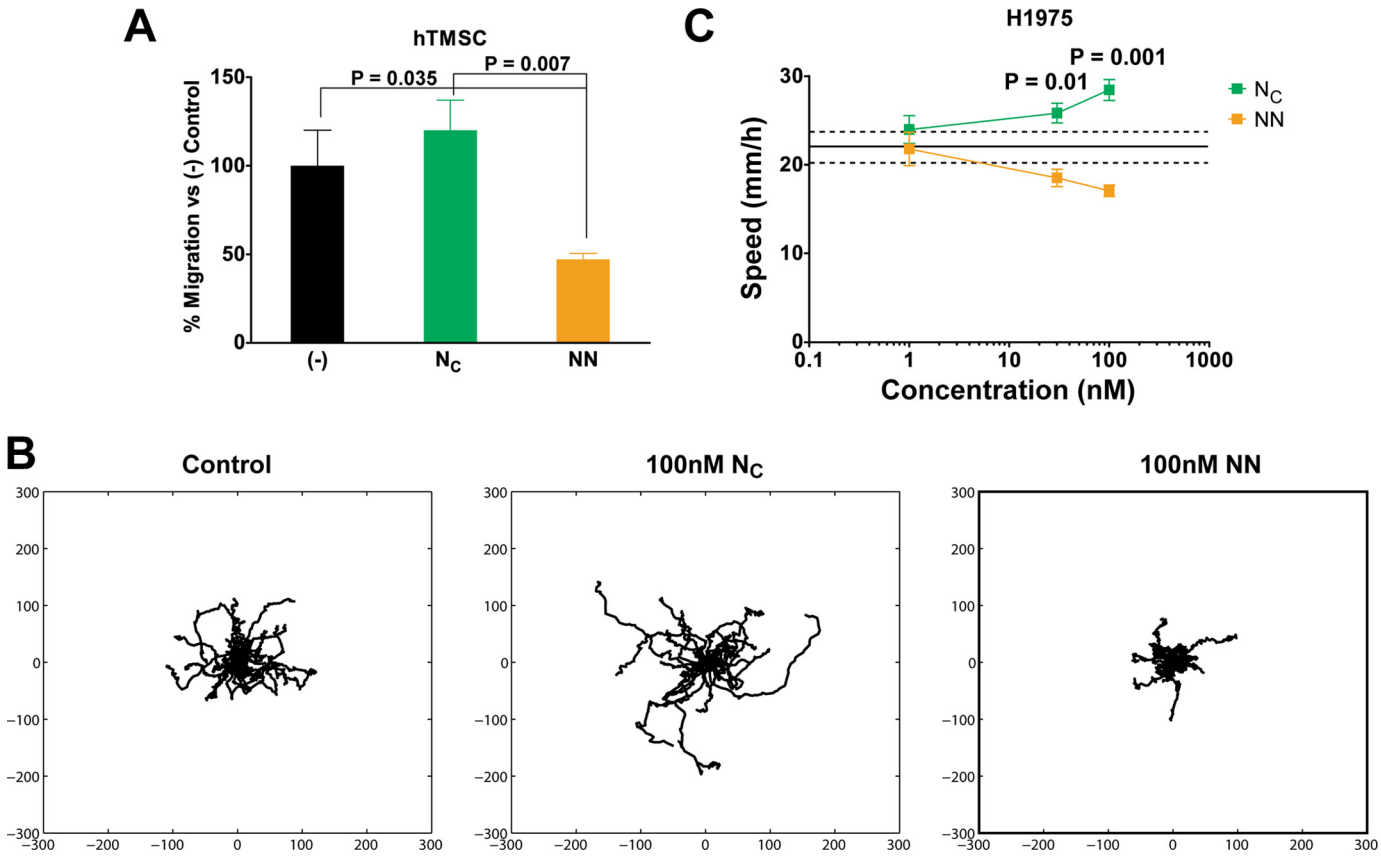

FIGURE 3. **Bivalent NN inhibits cell migration.** *A*, hTMSC on a transwell insert membrane were unstimulated (−) or stimulated by monovalent NRG (N_C) or bivalent NN, and cells migrating across the membrane after 18 h were quantified via SYTO 16 nuclear staining ($n = 3$). *B*, representative wind rose plots of H1975 cells stimulated for 12 h by control media, N_C, or NN are shown. *C*, quantitation of cell speed from H1975 single cell migration studies ($n = 30$) is shown. The *solid line* indicates untreated control cell mean speed, and the *dashed lines* indicate S.E, for control condition.

dose-dependent manner upon exposure to NN (supplemental Fig. S5).

Based on the evidence that bivalent NN is capable of inhibiting migration, we further hypothesized that NN may inhibit additional malignant phenotypes associated with HER3-HER2-driven signaling. When H3255 cells were dosed with NN over a 48-h period in serum-free media, we observed a decrease in cell number compared with untreated controls, whereas NRG (N_C) stimulation led to proliferation compared with controls (Fig. 4*A*). This result indicates that biased signaling via NN (Figs. 1*C* and 2*B*) results in suppression of malignant phenotypes.

We also examined potential proliferative effects in cells with lower reported expression levels of HER3 to assess the specificity and potency of NN in this setting. NSCLC line H1299, which expresses EGFR and low levels of HER2 and HER3 (41) and no HER4 (56) (supplemental Fig. S2), responded only weakly to NRG (N_C), even at high doses (supplemental Fig. S6). Predictably, the effect of NN on these cells was also muted; yet, at the highest dose administered, a significant reduction in proliferation compared with N_C was observed as was a decrease in cell number compared with untreated control (supplemental Fig. S6). Thus, even in cells that are not highly sensitive to NRG stimulation, we observed a differential effect of NN treatment, supportive of the hypothesis that NN can bias signaling via HER3 sequestration in many ErbB receptor contexts. However, clearly the most dramatic and potentially therapeutically relevant differential effects of NN treatment are observed in cell lines that respond most sensitively to NRG stimulation, as would be expected.

In furtherance of this last observation, we examined signaling and additional phenotypes in H1975 cells, which were previously shown to be highly sensitive to NRG stimulation (Fig. 3, *B* and *C*), and MDA-MB-453 cells, a breast carcinoma line that is also responsive to NRG (57). In these cells, NRG (N_C) enhanced proliferation of MDA-MB-453 cells in a dose-dependent manner, whereas NN suppressed proliferation and induced a reduction in cell number compared with control (supplemental Fig. S7*A*). These phenotypic effects could also be linked with differential phosphorylation of HER2 and HER3 by NRG (N_C) and NN (supplemental Fig. S7*B*). The appreciable levels of phosphorylation of HER2 and HER3 in these cells at high doses of NN could be caused by HER3-HER4 heterotypic or HER4 homotypic interactions, as cell stimulation conducted in the presence of a HER4-blocking antibody resulted in a near complete reduction of NN-induced phosphorylation of HER3 and HER2, whereas N_C-mediated phosphorylation was relatively unaffected (supplemental Fig. S7*C*).

H1975 cells responded more appreciably to N_C stimulation, with proliferation increased by 2–3-fold compared with controls when cells were maintained in serum-free conditions for 48 h (Fig. 4*B*). In stark contrast, NN inhibited proliferation significantly compared with N_C under these conditions (Fig. 4*B*),

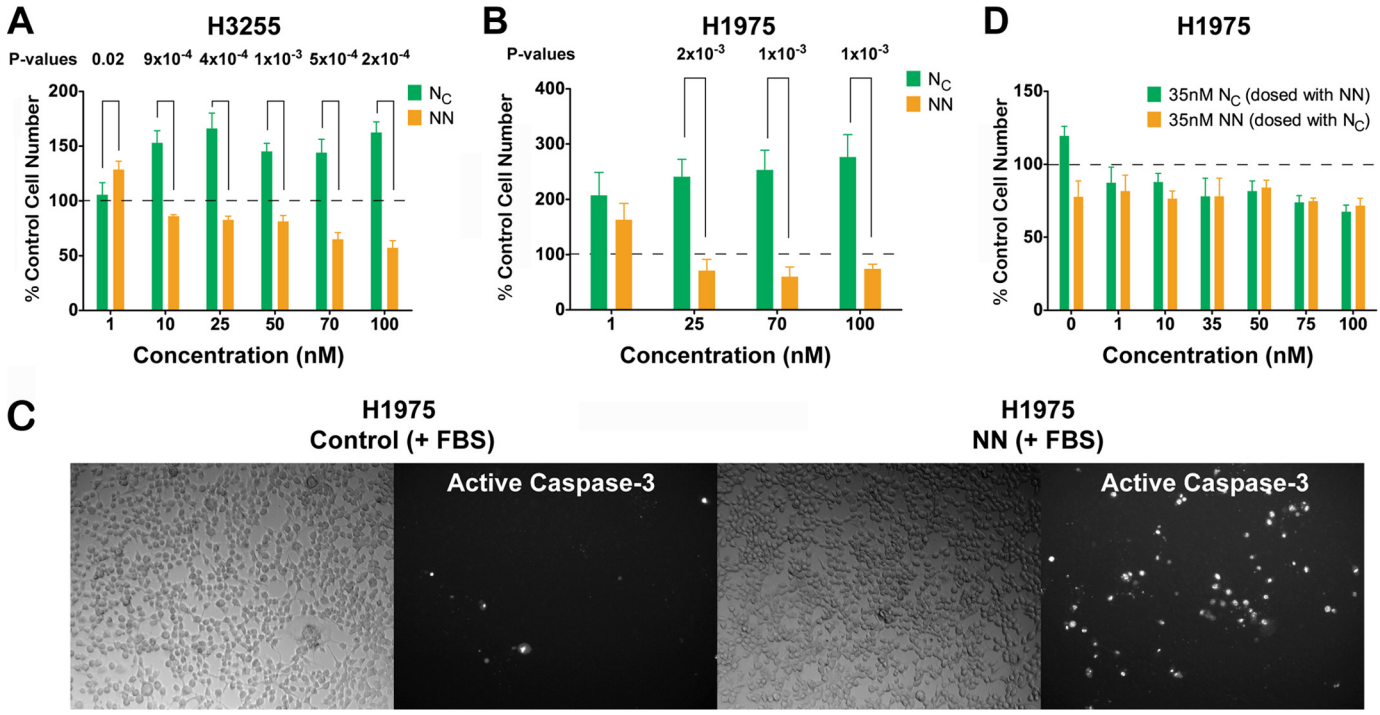

FIGURE 4. **Bivalent NN inhibits proliferation and increases apoptosis of cancer cells.** H3255 (*A*) and H1975 (*B*) cells were stimulated with monovalent NRG (N_C) or bivalent NN in serum-free conditions for 48 h. Cellular activity relative to untreated control (100%) was quantified using the CyQUANT assay ($n = 4$). *C*, H1975 cells were exposed to NN or control media in the presence of serum for 24 h and stained for activated caspase-3 (data representative of 2 independent experiments). *D*, H1975 cells, in 10% serum media, were simultaneously stimulated with either 35 nM monovalent NRG (N_C) or 35 nM bivalent NN and the indicated doses (on the *x* axis) of the other ligand for 48 h ($n = 5$, brightfield images to *left* of stained sections).

and NN treatment also resulted in a decrease in cell number compared with untreated controls. The disparate effects of native NRG and bivalent NN ligands on proliferation of H1975 cells were also observed in culture medium containing serum (supplemental Fig. S8). In the presence of serum, a source of ligands for EGFR, c-MET, and other receptor-tyrosine kinases expressed by H1975 cells, the effects of monovalent NRG (N_C) on proliferation were blunted compared with serum-free conditions. However, bivalent NN still suppressed proliferation of H1975 cells (supplemental Fig. S8), suggesting that HER3 is a central nexus for funneling proliferation signals in these cells in the presence of the multiple stimulants present in serum. The reduced cell numbers observed in the presence of NN compared with control cells were attributed in part to increased apoptosis in the presence of NN, as H1975 cells cultured in the presence of bivalent NN ligand exhibited a greater proportion of cells that stained positive for activated caspase-3 (Fig. 4*C*).

To determine whether the divergent phenotypic effects observed in H1975 cells could be attributed to both NN and NRG acting through the same binding site (HER3), we assessed cell proliferation in the presence of either monovalent N_C or bivalent NN and competing doses of the other ligand. 35 nM N_C-stimulated H1975 exhibited increased proliferation compared with unstimulated cells in media containing serum, as also shown in supplemental Fig. S8 (Fig. 4*D*). However, simultaneous co-stimulation with increasing doses of NN led to a decrease in proliferation (Fig. 4*D*). In contrast, 35 nM NN-stimulated cells, whereas exhibiting reduced proliferation compared with untreated control as previously shown (supplemental Fig. S8), did not proliferate in response to increasing (simultaneous) doses of N_C. This may have occurred due to a lack of receptor reorganization on the cell surface upon binding of N_C; if, as we hypothesize, HER3 receptors are sequestered together by NN, replacement of a NRG domain of NN by a native NRG via competition would seem unlikely to promote a change in the receptor association with its nearest neighbors.

Finally, the phenotypic effects observed in H1975 cells were also linked with differential HER2 and HER3 receptor phosphorylation profiles attributed to N_C and NN (supplemental Fig. S9). Although N_C induced dose-dependent increases in both pHER3 and pHER2, NN stimulation led to only slight induction of HER3 phosphorylation at high doses, whereas HER2 activation appeared to decrease in a dose-dependent manner. Intracellularly, both ERK1/2 and Akt were phosphorylated resultant from low doses of both N_C and NN in these cells (supplemental Fig. S9). However, whereas increased N_C dosage led to increased levels of pERK1/2 and pAkt, high doses of NN resulted in diminished phosphorylation of both intracellular proteins, mirroring the pattern observed for HER2 phosphorylation (supplemental Fig. S9). Thus, these data are supportive of the conclusion that bivalent NN interacts with surface HER3 receptors and sequesters them from participation in HER2-associated signaling complexes, leading to reduced HER2 phosphorylation. The reduction in HER2-mediated signaling then led to reduced activation of intracellular proteins (ERK1/2, Akt) that play important roles in cell proliferation, survival, and motility, and thus the cells exhibited reduced capacities in these activities, as shown in Figs. 3, *B* and *C* (migration), 4*D* (apoptosis), and 4, *B* and *C*, and supplemental Fig. S8 (proliferation). A similar phenomenon was also observed in H3255 cells, where

differential receptor phosphorylation (Fig. 1*C*) was linked to differential induction of intracellular signaling pathways (Fig. 2*B*) that led to differential phenotypic effects (Fig. 4*A*).

Thus, in multiple cell lines, we established that engineered bivalent NN induces differential HER receptor phosphorylation compared with native NRG. These directed receptor interactions, which are predictable based on knowledge of HER ligand-receptor affinity interactions, biased downstream signaling pathways, leading to unique and beneficial phenotypes.

DISCUSSION

The approach described here is a departure from traditional methods used to influence HER receptor signaling. Small molecule inhibitors target kinases, whereas antibody-based approaches target receptor ectodomains and ligands (5, 14, 29). Small molecule approaches also have risks of off-target toxicity, whereas antibody-based approaches are limited by affinity maxima, high dosing requirements, and relatively large molecular weights (~150 kDa) (58). Therapeutic options are further limited for HER3 as it lacks significant kinase activity; hence, we focused our attention on this important target and exploited this deficiency. Although it is arguably counterintuitive to silence a pathway by engaging the receptor with ligand, it is possible that, compared with function-blocking antibodies, bivalent ligands (particularly NN) may exhibit some therapeutic advantage; *e.g.* by engaging the receptors in more favorable steric associations for inhibiting interactions with other partners, altering internalization rates, or through improved tumor-penetrating properties.

Previous attempts to force hetero- and homodimerization of EGFR and HER2 showed altered proliferation and migration depending on the type of receptor dimer formed (59). However, that approach relied on expression of modified receptors with rapamycin binding domains to force particular receptor pairings. The approach we describe alters receptor interactions and biases signaling with an exogenous method that does not require genetic intervention. Another report describes exogenous application of a surface-bound dimeric EGF ligand for selective expansion of neural stem cells (60). In this study we demonstrate enhanced versatility of bivalent ligands by incorporating NRG moieties and provide a conceptually new application, inhibition of signaling. Furthermore, we establish the potential to selectively bias signaling in a particular cell type, based on its HER-family receptor expression profile, and to potentially apply bivalent ligands in a therapeutic context.

There are several possible mechanistic interpretations for how NN, which binds to HER3 (and HER4), inhibits receptor activation, downstream signaling, and phenotypic behaviors. A bias toward HER3 homotypic interactions by NN is arguably anticipated. Several lines of evidence support the idea that HER3 exists in a closely clustered state before ligand binding, possibly in association with HER4 (9, 35, 37, 38, 61, 62), and all cell lines used in this study exhibited low levels of HER4 compared with HER3 (supplemental Fig. S2). Hence, bivalent NN might be able to trap HER3 receptors, either linking them as dimers or possibly resulting in a concatenation of cross-linked dimers as shown in Fig. 1*B*. This interpretation is supported by two consistent observations in our studies, which is that biasing and/or inhibitory effects of NN increased with dose and that low doses of NN produced similar results to corresponding doses of native, monovalent NRG. At low NN doses, where HER3 receptors may not be saturated and/or complete concatenation may not occur, HER3 may still be available for interaction with HER2, as would be the case with stimulation by native NRG. Upon increasing the dose of NN, if the proposed hypothesis is true, complete concatenation or saturation of HER3 by NN would prevent interaction with HER2, and thus result in the differential signaling and phenotypic outcomes from NRG that were observed in this study. In this case, the efficacy of NN in biasing signaling would be dependent on the relative numbers and locations of HER receptors, disparities in which may explain the different effects observed in different cell lines with similar gross HER receptor profiles in this study. It is also notable that ligand-induced dimerization/homotypic association of HER3 has rarely been reported, especially in a cellular context (39, 62). Ligand binding is believed to unlock HER3 from the clustered, inhibited state, allowing it to find and associate with HER2 (or other partners). When HER3 partners with HER2, activation of signaling likely requires tetramers or higher order oligomers to overcome the kinase deficiency of HER3, although detailed structures and mechanisms of this activation process are still not clear (37, 39, 40). It is, therefore, possible that bivalent NN could link two HER3 receptors facing each other, leaving the dimerization face available for interaction with HER2 or other partners (*i.e.* instead of the concatenation with HER3, as shown in Fig. 1*B*). If such "solo, facing-each-other" dimers are indeed formed, they are likely constrained from proper (activating) interactions with HER2, as evidenced by the lack of HER3-mediated signaling observed in the presence of NN.

In contrast to the near-complete inhibition of receptor activation and signaling observed with NN, our more limited study of bivalent EE revealed that it activated cognate receptor EGFR and only partially biased activation away from HER2 (Fig. 1*E*). These results are consistent with a mechanistic model in which EE may opportunistically bind to a variety of pre-formed EGFR states (homodimers, oligomers, and heterodimers) that have been reported by others to exist in dynamic equilibrium on the cell surface (9, 42). Thus, EE may serve to stabilize dimers or concatamers (Fig. 1*D*) upon binding to homotypically pre-associated EGFR via both EGF moieties and also may act as a monomeric ligand upon binding to EGFR that is not homotypically pre-associated. It is also possible that EE induces a solo, facing-each-other dimer that leaves the dimerization face available for interaction with HER2.

Potential mechanistic interpretations notwithstanding, these studies suggest that a bivalent NN ligand could have therapeutic applications. Recent findings point to HER3 interactions with c-MET as a mechanism for therapeutic resistance after treatment with various chemotherapeutic agents (19, 55, 63). Furthermore, HER3- and/or HER4-mediated autocrine signaling may play an important role in certain types of ovarian cancer (64). In that regard inhibition of proliferation of H1975 cells by NN is particularly interesting, as H1975 express HER4 at detectable levels (55) and would thus presumably bind NN through both HER3 and HER4. HER4 responses can promote proliferation of breast (48) and lung (56) cancers; thus, the abil-

ity of NN to inhibit malignant phenotypes in cancer cells that co-express HER3 and HER4 is an encouraging observation. The therapeutic implications of the EGF-containing bivalent ligands are less clear. HER2 is implicated as an important partner in the pathogenesis of certain EGFR-overexpressing tumors (65), as HER2-EGFR dimers more strongly activate malignant signaling pathways compared with EGFR homodimers (66). As opposed to NN, EE and EN may bias signaling to alternative productive pathways, making them less promising to pursue as possible chemotherapeutics but of interest for future studies on phenotypes relevant for regenerative medicine. More broadly, bivalent ligands may be deployed as a new tool for dissecting the complex systems biology of the EGFR family in developmental biology, tissue regeneration, wound healing, and other physiological and pathophysiological processes (67).

Acknowledgments—We thank Eric Winer, Alan Wells, Forest White, David Stern, Doug Lauffenburger, and Matt Lazzara for helpful discussions and Matt Nugent for assistance with receptor binding studies.

REFERENCES

1. Olayioye, M. A., Neve, R. M., Lane, H. A., and Hynes, N. E. (2000) *EMBO. J.* **19,** 3159–3167
2. Burgess, A. W., Cho, H. S., Eigenbrot, C., Ferguson, K. M., Garrett, T. P., Leahy, D. J., Lemmon, M. A., Sliwkowski, M. X., Ward, C. W., and Yokoyama, S. (2003) *Mol. Cell* **12,** 541–552
3. Ciardiello, F., and Tortora, G. (2008) *N. Engl. J. Med.* **358,** 1160–1174
4. De, P., and Leyland-Jones, B. (2010) *J. Clin. Oncol.* **28,** 1091–1096
5. Schoeberl, B., Faber, A. C., Li, D., Liang, M. C., Crosby, K., Onsum, M., Burenkova, O., Pace, E., Walton, Z., Nie, L., Fulgham, A., Song, Y., Nielsen, U. B., Engelman, J. A., and Wong, K. K. (2010) *Cancer Res.* **70,** 2485–2494
6. Cardó-Vila, M., Giordano, R. J., Sidman, R. L., Bronk, L. F., Fan, Z., Mendelsohn, J., Arap, W., and Pasqualini, R. (2010) *Proc. Natl. Acad. Sci. U.S.A.* **107,** 5118–5123
7. Junttila, T. T., Akita, R. W., Parsons, K., Fields, C., Lewis Phillips, G. D., Friedman, L. S., Sampath, D., and Sliwkowski, M. X. (2009) *Cancer Cell* **15,** 429–440
8. Lindzen, M., Lavi, S., Leitner, O., and Yarden, Y. (2010) *Proc. Natl. Acad. Sci. U.S.A.* **107,** 12559–12563
9. Lemmon, M. A. (2009) *Exp. Cell Res.* **315,** 638–648
10. Linggi, B., and Carpenter, G. (2006) *Trends Cell Biol.* **16,** 649–656
11. Riese, D. J., 2nd, van Raaij, T. M., Plowman, G. D., Andrews, G. C., and Stern, D. F. (1995) *Mol. Cell. Biol.* **15,** 5770–5776
12. Schneider, M. R., and Wolf, E. (2009) *J. Cell. Physiol.* **218,** 460–466
13. Kochupurakkal, B. S., Harari, D., Di-Segni, A., Maik-Rachline, G., Lyass, L., Gur, G., Kerber, G., Citri, A., Lavi, S., Eilam, R., Chalifa-Caspi, V., Eshhar, Z., Pikarsky, E., Pinkas-Kramarski, R., Bacus, S. S., and Yarden, Y. (2005) *J. Biol. Chem.* **280,** 8503–8512
14. Baselga, J., and Swain, S. M. (2009) *Nat. Rev. Cancer* **9,** 463–475
15. Shi, F., Telesco, S. E., Liu, Y., Radhakrishnan, R., and Lemmon, M. A. (2010) *Proc. Natl. Acad. Sci. U.S.A.* **107,** 7692–7697
16. Campbell, M. R., Amin, D., and Moasser, M. M. (2010) *Clin. Cancer Res.* **16,** 1373–1383
17. Kruser, T. J., and Wheeler, D. L. (2010) *Exp. Cell Res.* **316,** 1083–1100
18. Amin, D. N., Sergina, N., Ahuja, D., McMahon, M., Blair, J. A., Wang, D., Hann, B., Koch, K. M., Shokat, K. M., and Moasser, M. M. (2010) *Sci. Transl. Med.* **2,** 16ra17
19. Turke, A. B., Zejnullahu, K., Wu, Y. L., Song, Y., Dias-Santagata, D., Lifshits, E., Toschi, L., Rogers, A., Mok, T., Sequist, L., Lindeman, N. I., Murphy, C., Akhavanfard, S., Yeap, B. Y., Xiao, Y., Capelletti, M., Iafrate, A. J., Lee, C., Christensen, J. G., Engelman, J. A., and Jänne, P. A. (2010) *Cancer Cell* **17,** 77–88
20. Ware, C. F., VanArsdale, S., and VanArsdale, T. L. (1996) *J. Cell. Biochem.* **60,** 47–55
21. Barbacci, E. G., Guarino, B. C., Stroh, J. G., Singleton, D. H., Rosnack, K. J., Moyer, J. D., and Andrews, G. C. (1995) *J. Biol. Chem.* **270,** 9585–9589
22. Moll, J. R., Ruvinov, S. B., Pastan, I., and Vinson, C. (2001) *Protein. Sci.* **10,** 649–655
23. Xue, C., Liang, F., Mahmood, R., Vuolo, M., Wyckoff, J., Qian, H., Tsai, K. L., Kim, M., Locker, J., Zhang, Z. Y., and Segall, J. E. (2006) *Cancer Res.* **66,** 1418–1426
24. Martin, A., Baker, T. A., and Sauer, R. T. (2005) *Nature* **437,** 1115–1120
25. Cho, H. S., and Leahy, D. J. (2002) *Science* **297,** 1330–1333
26. Warren, C. M., Kani, K., and Landgraf, R. (2006) *J. Biol. Chem.* **281,** 27306–27316
27. Iyer, A. K., Tran, K. T., Borysenko, C. W., Cascio, M., Camacho, C. J., Blair, H. C., Bahar, I., and Wells, A. (2007) *J. Cell. Physiol.* **211,** 748–758
28. Ogiso, H., Ishitani, R., Nureki, O., Fukai, S., Yamanaka, M., Kim, J. H., Saito, K., Sakamoto, A., Inoue, M., Shirouzu, M., and Yokoyama, S. (2002) *Cell* **110,** 775–787
29. Franklin, M. C., Carey, K. D., Vajdos, F. F., Leahy, D. J., de Vos, A. M., and Sliwkowski, M. X. (2004) *Cancer Cell* **5,** 317–328
30. Liu, H., Buus, R., Clague, M. J., and Urbé, S. (2009) *PLoS One* **4,** e5544
31. Wallasch, C., Weiss, F. U., Niederfellner, G., Jallal, B., Issing, W., and Ullrich, A. (1995) *EMBO J.* **14,** 4267–4275
32. Aguilar, Z., Akita, R. W., Finn, R. S., Ramos, B. L., Pegram, M. D., Kabbinavar, F. F., Pietras, R. J., Pisacane, P., Sliwkowski, M. X., and Slamon, D. J. (1999) *Oncogene* **18,** 6050–6062
33. van der Woning, S. P., and van Zoelen, E. J. (2009) *Biochem. Biophys. Res. Commun.* **378,** 285–289
34. Hutcheson, I. R., Goddard, L., Barrow, D., McClelland, R. A., Francies, H. E., Knowlden, J. M., Nicholson, R. I., and Gee, J. M. (2011) *Breast Cancer Res.* **13,** R29
35. Kani, K., Warren, C. M., Kaddis, C. S., Loo, J. A., and Landgraf, R. (2005) *J. Biol. Chem.* **280,** 8238–8247
36. Pinkas-Kramarski, R., Lenferink, A. E., Bacus, S. S., Lyass, L., van de Poll, M. L., Klapper, L. N., Tzahar, E., Sela, M., van Zoelen, E. J., and Yarden, Y. (1998) *Oncogene* **16,** 1249–1258
37. Jura, N., Shan, Y., Cao, X., Shaw, D. E., and Kuriyan, J. (2009) *Proc. Natl. Acad. Sci. U.S.A.* **106,** 21608–21613
38. Park, E., Baron, R., and Landgraf, R. (2008) *Biochemistry* **47,** 11992–12005
39. Berger, M. B., Mendrola, J. M., and Lemmon, M. A. (2004) *FEBS Lett.* **569,** 332–336
40. Bublil, E. M., Pines, G., Patel, G., Fruhwirth, G., Ng, T., and Yarden, Y. (2010) *FASEB J.* **24,** 4744–4755
41. Engelman, J. A., Jänne, P. A., Mermel, C., Pearlberg, J., Mukohara, T., Fleet, C., Cichowski, K., Johnson, B. E., and Cantley, L. C. (2005) *Proc. Natl. Acad. Sci. U.S.A.* **102,** 3788–3793
42. Chung, I., Akita, R., Vandlen, R., Toomre, D., Schlessinger, J., and Mellman, I. (2010) *Nature* **464,** 783–787
43. Hutchings, S. E., and Sato, G. H. (1978) *Proc. Natl. Acad. Sci. U.S.A.* **75,** 901–904
44. Oksvold, M. P., Skarpen, E., Lindeman, B., Roos, N., and Huitfeldt, H. S. (2000) *J. Histochem. Cytochem.* **48,** 21–33
45. Berkers, J. A., van Bergen en Henegouwen, P. M., and Boonstra, J. (1991) *J. Biol. Chem.* **266,** 922–927
46. Vieira, A. V., Lamaze, C., and Schmid, S. L. (1996) *Science* **274,** 2086–2089
47. Tamama, K., Fan, V. H., Griffith, L. G., Blair, H. C., and Wells, A. (2006) *Stem Cells* **24,** 686–695
48. Chuu, C. P., Chen, R. Y., Barkinge, J. L., Ciaccio, M. F., and Jones, R. B. (2008) *Mol. Cancer Res.* **6,** 885–891
49. Soler, M., Mancini, F., Meca-Cortés, O., Sánchez-Cid, L., Rubio, N., López-Fernández, S., Lozano, J. J., Blanco, J., Fernández, P. L., and Thomson, T. M. (2009) *Int. J. Cancer* **125,** 2565–2575
50. Sithanandam, G., Fornwald, L. W., Fields, J., and Anderson, L. M. (2005) *Oncogene* **24,** 1847–1859
51. Kumar, N., Afeyan, R., Kim, H. D., and Lauffenburger, D. A. (2008) *Mol. Pharmacol.* **73,** 1668–1678
52. Vadlamudi, R., Adam, L., Tseng, B., Costa, L., and Kumar, R. (1999) *Cancer*

Res. **59,** 2843–2846
53. Yang, C., Liu, Y., Lemmon, M. A., and Kazanietz, M. G. (2006) *Mol. Cell. Biol.* **26,** 831–842
54. Xia, W., Liu, L. H., Ho, P., and Spector, N. L. (2004) *Oncogene* **23,** 646–653
55. Yamada, T., Matsumoto, K., Wang, W., Li, Q., Nishioka, Y., Sekido, Y., Sone, S., and Yano, S. (2010) *Clin. Cancer Res.* **16,** 174–183
56. Starr, A., Greif, J., Vexler, A., Ashkenazy-Voghera, M., Gladesh, V., Rubin, C., Kerber, G., Marmor, S., Lev-Ari, S., Inbar, M., Yarden, Y., and Ben-Yosef, R. (2006) *Int. J. Cancer* **119,** 269–274
57. Crovello, C. S., Lai, C., Cantley, L. C., and Carraway, K. L., 3rd. (1998) *J. Biol. Chem.* **273,** 26954–26961
58. Imai, K., and Takaoka, A. (2006) *Nat. Rev. Cancer* **6,** 714–727
59. Muthuswamy, S. K., Gilman, M., and Brugge, J. S. (1999) *Mol. Cell. Biol.* **19,** 6845–6857
60. Nakaji-Hirabayashi, T., Kato, K., and Iwata, H. (2009) *Bioconjug. Chem.* **20,** 102–110
61. Tao, R. H., and Maruyama, I. N. (2008) *J. Cell Sci.* **121,** 3207–3217
62. Yang, S., Raymond-Stintz, M. A., Ying, W., Zhang, J., Lidke, D. S., Steinberg, S. L., Williams, L., Oliver, J. M., and Wilson, B. S. (2007) *J. Cell Sci.* **120,** 2763–2773
63. Wang, W., Li, Q., Yamada, T., Matsumoto, K., Matsumoto, I., Oda, M., Watanabe, G., Kayano, Y., Nishioka, Y., Sone, S., and Yano, S. (2009) *Clin. Cancer Res.* **15,** 6630–6638
64. Sheng, Q., Liu, X., Fleming, E., Yuan, K., Piao, H., Chen, J., Moustafa, Z., Thomas, R. K., Greulich, H., Schinzel, A., Zaghlul, S., Batt, D., Ettenberg, S., Meyerson, M., Schoeberl, B., Kung, A. L., Hahn, W. C., Drapkin, R., Livingston, D. M., and Liu, J. F. (2010) *Cancer Cell* **17,** 298–310
65. Lane, H. A., Beuvink, I., Motoyama, A. B., Daly, J. M., Neve, R. M., and Hynes, N. E. (2000) *Mol. Cell. Biol.* **20,** 3210–3223
66. Muthuswamy, S. K., Li, D., Lelievre, S., Bissell, M. J., and Brugge, J. S. (2001) *Nat. Cell Biol.* **3,** 785–792
67. Wiley, H. S., Shvartsman, S. Y., and Lauffenburger, D. A. (2003) *Trends Cell Biol.* **13,** 43–50